Coupling of Independent Electrochemical Reactions and Fluorescence at Closed
Bipolar Interdigitated Electrode Arrays

Wei Xu1, Chaoxiong Ma1, and Paul W. Bohn1,2\*

<sup>1</sup>Department of Chemistry and Biochemistry, University of Notre Dame, Notre Dame, IN 46556

<sup>2</sup>Department of Chemical and Biomolecular Engineering, University of Notre Dame, Notre Dame, IN 46556

<sup>\*</sup>Author to whom correspondence should be addressed, *pbohn@nd.edu* 

### **Abstract**

Electrochemical reactions occurring at the opposite ends of bipolar electrodes (BPEs) are necessarily coupled, enabling electron transfer events at one end to be read out optically, for example, by coupling to fluorigenic reactions at the other end. To explore the potential of this technique for studying multiple redox events, arrays of parallel BPE interdigitated electrode arrays (IDEAs) were fabricated and integrated with separate analytical and reporter microfluidic channels, respectively, in an closed BPE configuration. The apparatus was initially evaluated employing Fe(CN)<sub>6</sub>3/4- in the analytical channel coupled to weakly-emissive resazurin and strongly-emissive resorufin as the fluorigenic redox reporter pair. The device was then used to investigate a proton-coupled electron transfer reaction, hydroquinone (QH<sub>2</sub>) oxidation, in structures with an integrated pH modulation electrode (PME). A pH-sensitive dye, fluorescein, was co-introduced in the analytical channel to monitor PME modulation of solution pH, and its coupling to QH<sub>2</sub> oxidation, thereby permitting changes in solution pH, and consequently QH<sub>2</sub> oxidation rate, to be monitored directly in the analytical channel and compared to the fluorescence in the reporter channel. In addition, diffusion of OH generated at the PME produced a spatial pH profile that was visualized via fluorescein emission, and, because the oxidation of QH<sub>2</sub> at each BPE is strongly dependent on the local pH, via the coupled fluorigenic reaction at the opposite pole of the corresponding BPE digit in the reporter channel. Thus, BPE IDEAs support the coupling of independent redox reactions and the use of fluorescence imaging to explore a diverse set of spatially varying electrochemical phenomena realized in a variety of electrochemical geometries.

### Introduction

Bipolar electrochemistry has experienced a renaissance both in understanding the fundamental principles and applications in chemical analysis and electrochemical processing.<sup>[1]</sup>

Applications of bipolar electrochemistry span a wide range from material preparation and fabrication,<sup>[2]</sup> sensing and screening<sup>[3]</sup> to microswimmers<sup>[4]</sup> and bipolar electrode focusing.<sup>[5]</sup> In addition to their unique electrochemical characteristics, bipolar electrodes (BPEs) also derive utility from their form factor; they can be fabricated in a variety of sizes, shapes, and topological forms.

A bipolar electrode is an electronic conductor with no direct external connection, that is typically placed in direct contact with a fluid supporting an electric field, and that can be used to couple two distinct redox reactions at the two ends (poles) of the BPE.<sup>[6]</sup> The contact fluid is electrified by applying a voltage between two driving electrodes at opposite ends of the fluid medium. The resulting potential gradient maps onto the isopotential of the BPE creating interfacial potential differences between the opposite poles of the BPE and the electrolyte solution in contact with them. In contrast to working electrodes in a traditional three-electrode system, the potential difference between the electrode and the solution is determined by the magnitude of the electric field in solution and the axial length of the BPE along the field.<sup>[6]</sup> The unique construction and operating principles of the BPE imbue it with a number of interesting characteristics. For example, a large array can be easily controlled by a single voltage source.<sup>[7]</sup>

Bipolar electrochemistry can be accomplished in two primary electrode-solution topologies: open and closed.<sup>[1a]</sup> Open BPE arrangements place the electrode in an environment, for example a microchannel, in which both coupled reactions occur in the same solution environment. Open BPEs are capable of executing contact-free electrochemistry in a

microfluidic environment, which make it possible to control large electrode arrays with single voltage source<sup>[7]</sup> or to carry out electrochemistry at mobile electrodes.<sup>[8]</sup> Applications such as wire formation,<sup>[9]</sup> electrocatalyst screening,<sup>[3a, 10]</sup> compositional gradient generation,<sup>[11]</sup> and separation of charged analytes<sup>[12]</sup> have all been realized in open BPE structures.

In contrast, closed BPE systems involve a single BPE in contact with physically separate, chemically distinct solutions connected to the anodic and cathode poles of the BPE. Because there is no fluid path to provide electrical communication between the anodic and cathodic poles, the two half reactions at the poles of the BPE can only be coupled by electron transport through the BPE.<sup>[13]</sup> The advantage of using a closed BPE is that separation is achieved between the two redox systems, which eliminates possible interferences between them. Since the closed BPE is analogous to two electrochemical cells in series,<sup>[14]</sup> remote control or detection can be performed. Closed BPE-based carbon-fiber microelectrodes<sup>[13]</sup> and fluorescence coupling detection<sup>[15]</sup> are good examples of applications of closed BPE systems.

Because BPEs do not require direct electric connection, and large arrays of BPEs can be controlled simultaneously with a single voltage source, BPEs present intriguing possibilities for electroanalytical work. For example, they can utilize optical readout by coupling the analytical redox reaction at one pole to a fluorigenic (*e.g.* dark-to-emissive transition) redox process at the other pole, thereby combining the low-background of photon emission measurements with the attractive features of BPEs for supporting redox reactions. [16] Furthermore, exploiting closed BPE systems it is possible to arrange for the light emission measurement to be carried out remote from the analytical redox process, greatly simplifying experimental design. Realizing this principle, Crooks and coworkers demonstrated coupling between a non-fluorescent electrochemical reaction such as benzyl viologen reduction and electrogenerated

chemiluminescence (ECL) in Ru(bpy)<sub>3</sub><sup>2/3+</sup>/tri-*n*-propylamine.<sup>[17]</sup> Measuring the ECL light intensity neatly solves the problem associated with direct measurement of current flowing through the BPE.<sup>[18]</sup> Alternatively, electrochemical reactions that are fluorogenic or quench fluorescence are also good choices. Zhang and co-workers reported fluorescence-enabled electrochemical microscopy (FEEM) based on coupling to fluorogenic reactions, which enabled them to visualize electrochemical signals on a parallel array of vertically oriented BPEs simultaneously.<sup>[15, 19]</sup> Thus, by combining the advantages of BPEs and optical sensing and working in parallel on large arrays of BPEs simultaneously, they were able to use BPE-based optical sensing to achieve spatially- and temporally-resolved parallel electrochemical imaging.<sup>[20]</sup>

Chemical sensing and analysis in microfluidic systems have been widely studied due to attendant benefits, such as low cost, low sample consumption and portability. [21] Also, microfluidic systems use small volumes of chemicals, can achieve high sensitivity, [22] and can integrate multiple processes, [23] so they are well-suited for incorporation of BPE-based electroanalytical determinations and electrochemical processing. Here, we explore a microfluidically-integrated closed-BPE arrays containing multiple parallel BPE digits interdigitated with working (WE) and quasi-reference (QRE) electrodes and covered by two separate microchannels at the opposing poles, **Fig. 1**. This geometry enables high sensitivity redox cycling of analytical redox reactions to be coupled to remote fluorescence readout. As shown in **Fig. 1**, separate analytical and reporter microchannels work in tandem, to implement these BPE-coupled reactions. Weakly-emissive resazurin, which can be reduced to fluorescent resorufin, [24] is employed as fluorigenic reporter reaction. The interdigitated BPE device architecture has been evaluated using direct electron transfer, employing Fe(CN)<sub>6</sub><sup>3/4-</sup>, and by characterizing the pH-dependent oxidation of hydroquinone (QH<sub>2</sub>) to benzoquinone (Q). In the

latter pH-dependent reaction, pH gradients directly impact local redox reaction rates. BPE arrays permit the simultaneous measurement of both local pH (through a co-introduced pH-sensitive dye in the analytical channel) and QH<sub>2</sub> oxidation rate – through the BPE-coupled resazurin/resorufin reaction. These measurements have direct implications for the use of multiple BPE arrays for parallel, high-throughput detection schemes, such as those needed for high bandwidth electrochemical detection in molecular separations. [25]

#### **Results and Discussion**

Coupled Redox Cycling Events Enabled by Closed BPE. Figure 1 shows the layout of the BPE microfluidic device used in these studies. The arrangement consists of two powered electrodes, a working electrode (WE) and a quasi-reference electrode (QRE), controlled by a potentiostat. The WE and QRE are each bridged by an array of 15 parallel microband electrodes in an interdigitated electrode array (IDEA) arrangement on each end to form WE/BPE and QRE/BPE IDEAs. Two microchannels, an analytical channel and a reporter channel, are filled with the analyte and a fluorigenic reporter couple - resazurin/resorufin in the present instance — and placed over the analytical and reporter channels respectively. This design enhances coupling efficiency between the powered electrodes and the BPE array and simplifies the alignment with the microchannels. In addition, physically separating the analyte from the reporter in two channels reduces the possibility of interference or cross-talk.

In cyclic voltammetry (CV) as typically executed, a time-varying sawtooth potential is applied between WE and QRE. However, addition of the interdigitated BPE array integrated with the WE and QRE changes the operation significantly. When an appropriate potential is applied across WE and QRE, redox reactions on the WE can induce a counter-reaction on the

corresponding digit of the integrate BPEs array in the analytical channel. [14] Similarly, in the closed BPE configuration, reactions at the QRE/BPE pole in the reporter channel are required to balance the WE/BPE reactions in the analytical channel. As a result, reactions at the opposing ends of each BPE are coupled in order to maintain charge balance on the floating BPEs. The coupling of these reactions results in a deterministic relationship among the redox reactions at the four electrode surfaces: WE, BPE<sub>WE</sub>, BPE<sub>QRE</sub>, and QRE, that is summarized in **Table 1** (where BPE<sub>WE</sub> and BPE<sub>QRE</sub> refer to the interdigitated BPE at the WE and QRE ends, respectively).

To test these simple mechanistic ideas about reaction coupling, initially Fe(CN) 63/4- and resorufin were introduced into the analytical channel and reporter channel, respectively. The voltammetry was recorded while the WE was scanned from -1.0 V to 1.0 V in the absence of supporting electrolyte (SE), which was not used, because redox reactions of H<sub>2</sub>O can interfere with those of the analyte, an effect which becomes increasingly severe at higher ionic strength. The results of CV experiments conducted with  $Fe(CN)_6^{3-}$  are shown in Fig. 2, and the corresponding fluorescence images and time/potential behavior for Fe(CN)<sub>6</sub><sup>4-</sup> are shown in Fig. S1. Figure 2 shows that the fluorescence in the reporter channel is strongly correlated with the applied potential at the WE, with applied potentials negative of the equilibrium potential,  $E_{eq}$ , at WE corresponding to maximum fluorescence emission in the reporter channel. The fluorescence response is also in good agreement with the redox current from the CVs (Fig. S3), further supporting the validity of their use to monitor the redox reactions. When  $E \le E_{eq}$  is applied to the WE,  $Fe(CN)_6^{3-}$  is reduced to  $Fe(CN)_6^{4-}$ , and the corresponding oxidation reaction occurs on the adjacent BPEs in the analytical channel. Conservation of charge dictates that the electrons produced at the BPEwe are transferred and consumed at the BPEore in a reduction reaction in the reporter channel. Since resazurin is available in the reporter channel, and it can be readily reduced to highly fluorescent resorufin, the change of the fluorescence intensity at the BPE<sub>QRE</sub> correlates directly with the rate of  $Fe(CN)_6^{3-}$  reduction at the WE. Two other features of **Fig. 2** are noteworthy. First, the magnitude of the fluorescence intensity change increases with increasing concentration of  $Fe(CN)_6^{3-}$  in the analytical channel at the scan rate of 3.0V/s, a fast scan rate being used to minimize crosstalk of the BPEs in the reporter channels. Second, the rapid scan rate is likely responsible for the other notable feature, the asymmetry in the shape of the fluorescence potential response, which is not observed at low scan rate (**Fig. S3**)

The potential-dependent change in fluorescence intensity in the reporter channel is quite repeatable, and the fluorescence response at the BPE<sub>QRE</sub> and the QRE are out of phase with each other (**Table 1** and **Fig. S2**). As shown in **Figs. 2** and **S1**, the magnitude of the fluorescence change scales monotonically with the concentration of  $Fe(CN)_6^{3/4}$ . Although a quantitative relationship between the fluorescence and concentration of  $Fe(CN)_6^{3/4}$  has not been established in this experiment, the results show that redox reactions of  $Fe(CN)_6^{3/4}$  at concentrations as low as 10  $\mu$ M can be monitored by fluorescence with good signal-to-noise ratio. In addition, the variation of the fluorescence on 15 electrodes (**Fig. S2**) in the BPE array is  $\sim \pm 5\%$ , enabling the study of multiple reactions as a function of position within the analytical channel (*vide infra*).

It is interesting to note that the reporter channel fluorescence response to applied potential at the WE is similar between reduction of  $Fe(CN)_6^{3-}$  and oxidation of  $Fe(CN)_6^{4-}$ , *cf.* **Figs. 2** and **S1**. The reactions given in Table 1 and the spatial intensity variation shown in **Fig. S2** indicate efficient coupling of redox processes at the IDEAs, both in the analytical and reporter channels, since the IDEA geometry allows fast diffusion of  $Fe(CN)_6^{3/4-}$  between BPE<sub>WE</sub> and WE in the analytical channel and resazurin/resorufin between the BPE<sub>ORE</sub> and QRE in the reporter channel.

These results demonstrate the efficient coupled redox cycling of two separate redox reactions in two different spatial locations – a phenomenon that is only possible through the closed BPE geometry.

Closed BPE Proton-Coupled Electron Transfer. The results above show that coupling of separate redox cycling events on BPE IDEAs allows concentration-dependent monitoring of redox reactions by fluorescence. Next, the device was employed to study the effect of solution pH on a proton-coupled electron transfer (PCET) reaction, the oxidation of hydroquinone (QH<sub>2</sub>) to benzoquinone (Q),

$$QH_2 \longrightarrow Q + 2H^+ + 2e^-$$
 (1)

Since this reaction involves H<sup>+</sup>, it is strongly dependent on solution pH, *i.e.* oxidation of QH<sub>2</sub> is facilitated at higher pH. In addition, changes in solution pH can be monitored by a pH-sensitive dye, fluorescein, which exhibits strong fluorescence in its basic form, but much weaker emission in the acidic form with emission intensity changes occurring over the range of pH 4 to 10, <sup>[26]</sup> thus enabling two-channel fluorescence measurements in both analytical (monitoring H<sup>+</sup>) and reporter (monitoring e<sup>-</sup> transfer) channels.

To study the response of the closed BPE device to PCET reactions, 10 µM fluorescein and 10 mM QH<sub>2</sub> were added to the analytical channel at different pH values, and CVs were obtained from -0.8 V to +0.8 V while monitoring the fluorescence in both analytical and reporter channels. **Figure 3(a)** shows the fluorescence intensity observed on the BPE<sub>QRE</sub> IDEA in the reporter channel while scanning the potential applied to the WE. Similar to the oxidation of Fe(CN)<sub>6</sub><sup>4-</sup> (**Fig. S1**), the reduction/oxidation of Q/QH<sub>2</sub> on the WE produces a pH-dependent fluorescence maximum/minimum at the BPE<sub>QRE</sub> in the reporter channel. These fluorescence responses as well as their dependence on the solution pH are consistent with the redox reactions at WE, as

indicated by the corresponding CV curves in **Fig. S4**. Since the oxidation of  $QH_2$  to Q produces  $H^+$ , increasing the analytical channel pH shifts  $E_{eq}$  for  $QH_2/Q$  and is accompanied by an increase in the maximum fluorescence intensity in the reporter channel, because the BPE $_{QRE}$  reaction reports on the extent of the  $e^+$  transfer reaction. In contrast, **Fig. 3(b)** shows the change in fluorescence intensity as a function of applied potential in the analytical channel resulting from the pH-dependent emission of fluorescein. Changing solution pH in the analytical channel obviously leads to a different response. In contrast to the reporter channel behavior lower initial pH (minimal fluorescein emission) is accompanied by larger changes in fluorescence at the BPE $_{WE}$ , as the oxidation of  $QH_2$  to Q generates  $H^+$ , thereby lowering the local pH and decreasing the fluorescein emission intensity. Because pH 7 is near the mid-point of the pH-dependent fluorescein response range (pH 4-10) fluorescein responds most sensitively to changes of solution pH near pH 7. These results demonstrate the capability of the BPE device for simultaneously monitoring the changes in local concentrations of multiple reactants in coupled redox cycling reactions in different locations.

As an alternative to changing pH by introducing buffered solutions to the microchannels, it is possible to electrochemically modulate pH *in situ* using a pH modulating electrode (PME), *viz*. **Fig. 1(b)**.<sup>[27]</sup> As shown in **Fig. 4(a)** (black curve), the fluorescein emission intensity in the analytical channel increases with more negative potentials applied to the PME, consistent with the reduction of H<sub>2</sub>O, which occurs with the generation of OH<sup>-</sup>, thus increasing pH. This modulation of solution pH by the PME is coupled to the redox reaction of QH<sub>2</sub>/Q on the WE/BPEs as monitored by fluorescence in both analytical and reporter channels. Similar to the results in **Fig. 3**, a cathodic potential applied to the WE leads to increased fluorescence intensity at the BPE<sub>QRE</sub> IDEA in the reporter channel, but decreased intensity at the BPE<sub>WE</sub> in the

analytical channel. The amplitudes of both changes depend on the potential at the PME. More negative PME potentials produce a large change in reporter channel fluorescence, as shown in **Fig. 4(b)**, consistent with increased analytical channel pH that facilitates the oxidation of QH<sub>2</sub>. Similar to **Fig. 3(b)**, the amplitude of the fluorescence change in the analytical channel, blue squares in **Fig. 4(a)**, decreases at more negative PME potential, since the original solution at pH 7 is at the optimum sensitivity point. These results demonstrate the modulation of solution pH by the PME, its effect on the oxidation of QH<sub>2</sub>, and how these effects can be simultaneously monitored by fluorescence in the closed BPE device.

Parallel Sensing. Another possibility raised by these observations is to employ the closed BPE device to monitor multiple redox reactions simultaneously for parallel sensing by fluorescence imaging. The above results demonstrate electrochemical modulation of solution pH and its influence on the oxidation of QH<sub>2</sub>-based measurements at a single BPE digit. The change of solution pH at the BPE digits relies largely on the diffusion of OH- generated at the PME in the analytical channel. Thus, application of a negative potential at the PME produces a pH gradient with spatial and time dependences indicated by the movement of a band of increased fluorescence across the individual BPE digits. This pH gradient was employed to investigate the applicability of the closed BPE IDEA for parallel sensing. Figure 5 shows the fluorescence intensity of fluorescein in the analytical channel after a 15 s potential pulse of -1.0 V applied to the PME. A peak in emission intensity varying with time was observed at all BPE<sub>WE</sub> digits. The increase of the fluorescence intensity is attributed to the diffusion of OH<sup>-</sup> from the PME surface, whereas its decay can arise from a combination of diffusion of H<sup>+</sup> generated at the CE, as well as a small amount of photobleaching of the dye. The shift of the time at which maximum intensity is achieved at different BPE<sub>WE</sub> digits, Fig. 5 inset, reflects the difference in transit times required

for OH to arrive at each BPEWE digit.

Furthermore, since the oxidation of QH<sub>2</sub> is strongly pH sensitive, as demonstrated above, the extent of QH<sub>2</sub>/Q reaction at each BPE should depend on its distance to the PME and should also vary with time. This dependence was studied by monitoring the fluorescence behavior in the reporter channel. The fluorescence response of three representative BPE<sub>ORE</sub> digits, numbered I, II and III in order of distance from the PME, is given in Fig. 6, indicating obviously different time dependence. A decay of the fluorescence intensity with time was seen for the BPE (I), whereas an increase was seen for the BPE (III). In contrast, the fluorescence response initially increased then decreased at the middle BPE (II). This variation of fluorescence in the reporter channel with time reflects the change in pH in the analytical channel through its effect on the Q/QH<sub>2</sub> redox reaction, agreeing with the pH gradient observed in Fig. 5. These results demonstrate that modulation of solution conditions on the BPE array can be used to purposeful effect, here producing reactions with reactant of varying concentrations, which are simultaneously monitored by fluorescence imaging. Similar devices might be employed for studying multiple reactions with different reactants or reactants of different concentrations in parallel multiple sensing schemes.

### **Conclusions**

We explored the behavior of a device employing a closed bipolar electrode array integrated with working and quasi-reference electrodes in interdigitated electrode arrays in separate microchannels capable of coupling separate redox cycling reactions. Analytical reactions were amplified by redox cycling in one microchannel, while a fluorigenic reaction was cycled in a separate reporter channel enabling the detection of the analytical reaction through fluorescence

imaging. Separate electrochemical cycling events were thus coupled to each other by the bridged BPEs without direct contact. This concept was first characterized by using  $Fe(CN)_6^{3/4}$  analyte and resazurin/resorufin as the fluorigenic reporter reaction. The closed BPE IDEA architecture enables an unusual operating mode in which the fluorescence intensity observed in the reporter channel is linked to the concentration of analyte, here  $Fe(CN)_6^{3/4}$ , in the analytical channel through the number of charge-transfer event occurring on the BPE<sub>WE</sub>.

In a second model application, the device was used together with the Q/QH<sub>2</sub> redox couple, which exhibits proton-coupled electron transfer, to explore how the effects of solution pH in the analytical channel would manifest themselves through fluorescence in the reporter channel. As expected high pH in the analytical channel favors the oxidation of QH<sub>2</sub> to Q. In addition, solution pH in the analytical channel was monitored optically by using a pH-sensitive dye, fluorescein, permitting a dual fluorescence measurement in two separate channels to report independently on H<sup>+</sup> concentration (fluorescein in the analytical channel) and e<sup>-</sup> transfer (resazurin/resorufin in the reporter channel).

In the final application an upstream PME was incorporated in the analytical channel and water electrolysis was used to establish *in situ* control of the solution pH. The OH<sup>-</sup> generated by a negative potential applied at the PME formed a pH gradient downstream of the channel. In this configuration the presence of multiple BPE digits at distinct spatial locations was exploited to study multiple reactions under different conditions, *e.g.* pH, at each BPE digit simultaneously. Spatiotemporal variation of fluorescence in the reporter channel reports on QH<sub>2</sub> oxidation in the analytical channel, consistent with the pH profile generated in the analytical channel.

Taken together these results illustrate how the closed BPE architecture can be used to accomplish a powerful set of new analytical capabilities. It supports the spatially distributed

coupling of independent redox cycling events; it permits independent fluorescence intensity measurements to report on multiple reaction participants; and the distributed BPE IDEA array allows the spatial distribution of electrochemically active species to be imaged *in situ*, These strategies simplify the coupling of analytically useful redox reactions in one channel with a physically separate and chemically distinct sensing reaction. They also represent promising new approaches for high sensitivity, low-cost detection applications in chip-based microfluidic devices.

## **Experimental Section**

Chemicals and Materials. Hydroquinone (Alfa Aesar), resazurin (Sigma-Aldrich), and fluorescein (Fluka) were used as received. Microchannel masters were fabricated on *p*-type <100> silicon wafers (Montco Silicon Technology). SU-8 photoresist and developer were obtained from Microchips Inc. Poly(dimethylsiloxane) (PDMS) (Sylgard 184, Dow Corning) was used to fabricate microchannels for the device. AZ-5214E and AZ-917MIF (AZ Electronic Materials) were used as photoresists and developer for electrode patterning on glass slides (Propper Manufacturing). All reagents were analytical grade.

Device Fabrication. Microchannels were fabricated by photolithography and soft lithography with PDMS over a silicon/photoresist master. SU-8 2010 was spun on a piranha cleaned p-type <100> silicon wafer at 1000 rpm to make a thin layer of photoresist. After baking and exposure, the pattern was developed in SU-8 developer. Then, PDMS was poured over the obtained silicon/SU-8 master, cured at 65°C for at least 3 h, then peeled off the silicon wafer. The sizes of the channels were characterized by a profilometer (Dektak). 100 nm thick metal (95 nm Au over 5 nm Cr) electrodes were deposited on glass slides by thermal evaporation after

patterning with photolithography using AZ-5214 and photoresist liftoff in an acetone bath. The BPE arrays on glass included 15 parallel BPEs, each of which was 10 µm wide and 12 mm long, separated by 30 µm. Driving electrodes (WE and QRE) were patterned in an interdigitated arrangement with the BPEs to provide redox cycling possibilities as well as to simplify the alignment of electrodes with the microchannels. A single PME was placed 500 µm away from the BPE array. Microchannels were fabricated to be 8 µm in depth, 200 µm in width, and 15 mm in length with reservoirs at both ends. The analytical microchannel covered both PME and the interdigitated area of the coupled BPE/WE, while the reporter microchannel was placed over the interdigitated BPE/QRE.

Electrochemical and Fluorescence Measurements. Electrochemical measurements were performed on a commercial potentiostat (CHI 842C, CH Instruments). Cyclic voltammetry was performed at the WE with potential ranging from -1.0 V to +1.0 V at a scan rate of 2-3 V/s to drive the redox reaction. Fluorescence intensity changes were monitored on an epifluorescence microscope (IX-71, Olympus, PA) equipped with a X-Cite 120 PC illumination system (Exfo, Canada) and filter set (Chroma Technology Inc., VT). The fluorescence data were collected by an electron-multipled CCD camera (PhotonMax512, Princeton Instruments, NJ) at rate of 6 frames per second.

## Acknowledgement

This work was supported by the Department of Energy Office of Basic Energy Sciences through grant DE FG02 07ER15851 (WX) and by the National Science Foundation grant NSF1404744 (CM).

## Reference

- a) S. E. Fosdick, K. N. Knust, K. Scida, R. M. Crooks, *Angew Chem Int Edit* 2013, 52, 10438-10456;
   b) G. Loget, D. Zigah, L. Bouffier, N. Sojic, A. Kuhn, *Accounts Chem Res* 2013, 46, 2513-2523.
- a) J. C. Bradley, H. M. Chen, J. Crawford, J. Eckert, K. Ernazarova, T. Kurzeja, M. D. Lin, M. McGee, W. Nadler, S. G. Stephens, *Nature* 1997, 389, 268-271; b) C.
  Warakulwit, T. Nguyen, J. Majimel, M. H. Delville, V. Lapeyre, P. Garrigue, V. Ravaine, J. Limtrakul, A. Kuhn, *Nano Lett* 2008, 8, 500-504; c) C. Ulrich, O. Andersson, L.
  Nyholm, F. Bjorefors, *Angew Chem Int Edit* 2008, 47, 3034-3036.
- [3] a) S. E. Fosdick, R. M. Crooks, J Am Chem Soc 2012, 134, 863-866; b) M. S. Wu, G. S. Qian, J. J. Xu, H. Y. Chen, Anal Chem 2012, 84, 5407-5414; c) M. S. Wu, D. J. Yuan, J. J. Xu, H. Y. Chen, Chem Sci 2013, 4, 1182-1188.
- [4] a) Y. Wang, R. M. Hernandez, D. J. Bartlett, J. M. Bingham, T. R. Kline, A. Sen, T. E.
   Mallouk, *Langmuir* 2006, 22, 10451-10456; b) G. Loget, A. Kuhn, *J Am Chem Soc* 2010, 132, 15918-15919; c) J. Wang, K. M. Manesh, *Small* 2010, 6, 338-345.
- [5] a) R. K. Perdue, D. R. Laws, D. Hlushkou, U. Tallarek, R. M. Crooks, *Anal Chem* 2009, 81, 10149-10155; b) D. Hlushkou, R. K. Perdue, R. Dhopeshwarkar, R. M. Crooks, U. Tallarek, *Lab Chip* 2009, 9, 1903-1913.
- [6] F. Mavre, R. K. Anand, D. R. Laws, K. F. Chow, B. Y. Chang, J. A. Crooks, R. M. Crooks, Anal Chem 2010, 82, 8766-8774.
- [7] K. F. Chow, F. Mavre, J. A. Crooks, B. Y. Chang, R. M. Crooks, *J Am Chem Soc* 2009, 131, 8364-8365.
- [8] a) D. Kagan, P. Calvo-Marzal, S. Balasubramanian, S. Sattayasamitsathit, K. M.
  Manesh, G. U. Flechsig, J. Wang, *J Am Chem Soc* 2009, *131*, 12082-12083; b) J. Wu,
  S. Balasubramanian, D. Kagan, K. M. Manesh, S. Campuzano, J. Wang, *Nat Commun* 2010, *1*.

- [9] a) J. C. Bradley, J. Crawford, K. Ernazarova, M. McGee, S. G. Stephens, *Adv Mater* 1997, 9, 1168-1171; b) M. Wood, B. Zhang, *ACS Nano* 2015, 9, 2454-2464.
- [10] S. E. Fosdick, S. P. Berglund, C. B. Mullins, R. M. Crooks, *Anal Chem* **2013**, *85*, 2493-2499.
- [11] a) S. Ramakrishnan, C. Shannon, *Langmuir* 2010, *26*, 4602-4606; b) R. Ramaswamy, C. Shannon, *Langmuir* 2011, *27*, 878-881.
- [12] a) D. R. Laws, D. Hlushkou, R. K. Perdue, U. Tallarek, R. M. Crooks, *Anal Chem* 2009, 81, 8923-8929; b) E. Sheridan, K. N. Knust, R. M. Crooks, *Analyst* 2011, 136, 4134-4137.
- [13] J. P. Guerrette, S. M. Oja, B. Zhang, *Anal Chem* **2012**, *84*, 1609-1616.
- [14] J. T. Cox, J. P. Guerrette, B. Zhang, *Anal Chem* **2012**, *84*, 8797-8804.
- [15] J. P. Guerrette, S. J. Percival, B. Zhang, *J Am Chem Soc* **2013**, *135*, 855-861.
- [16] C. X. Ma, L. P. Zaino, P. W. Bohn, *Chem Sci* **2015**, *6*, 3173-3179.
- [17] a) W. Zhan, J. Alvarez, R. M. Crooks, J Am Chem Soc 2002, 124, 13265-13270; b) B. Y. Chang, K. F. Chow, J. A. Crooks, F. Mavre, R. M. Crooks, Analyst 2012, 137, 2827-2833.
- [18] F. Mavre, K. F. Chow, E. Sheridan, B. Y. Chang, J. A. Crooks, R. M. Crooks, Anal Chem 2009, 81, 6218-6225.
- [19] S. M. Oja, J. P. Guerrette, M. R. David, B. Zhang, *Anal Chem* **2014**, *86*, 6040-6048.
- [20] K. F. Chow, F. Mavre, R. M. Crooks, J Am Chem Soc 2008, 130, 7544-7545.
- [21] B. Kuswandi, Nuriman, J. Huskens, W. Verboom, Anal Chim Acta 2007, 601, 141-155.
- [22] G. M. Whitesides, *Nature* **2006**, *442*, 368-373.
- [23] D. Erickson, D. Q. Li, *Anal Chim Acta* **2004**, *507*, 11-26.
- [24] W. L. Xu, H. Shen, Y. J. Kim, X. C. Zhou, G. K. Liu, J. Park, P. Chen, *Nano Lett* 2009, 9, 3968-3973.

- [25] a) D. B. Gunasekara, J. M. Siegel, G. Caruso, M. K. Hulvey, S. M. Lunte, *Analyst* 2014, 139, 3265-3273; b) B. G. Lucca, S. M. Lunte, W. K. T. Coltro, V. S. Ferreira, *Electrophoresis* 2014, 35, 3363-3370.
- [26] a) M. M. Martin, L. Lindqvist, J Lumin 1975, 10, 381-390; b) H. Diehl, R. Markuszewski, Talanta 1989, 36, 416-418.
- [27] N. M. Contento, P. W. Bohn, Biomicrofluidics 2014, 8, 044120.

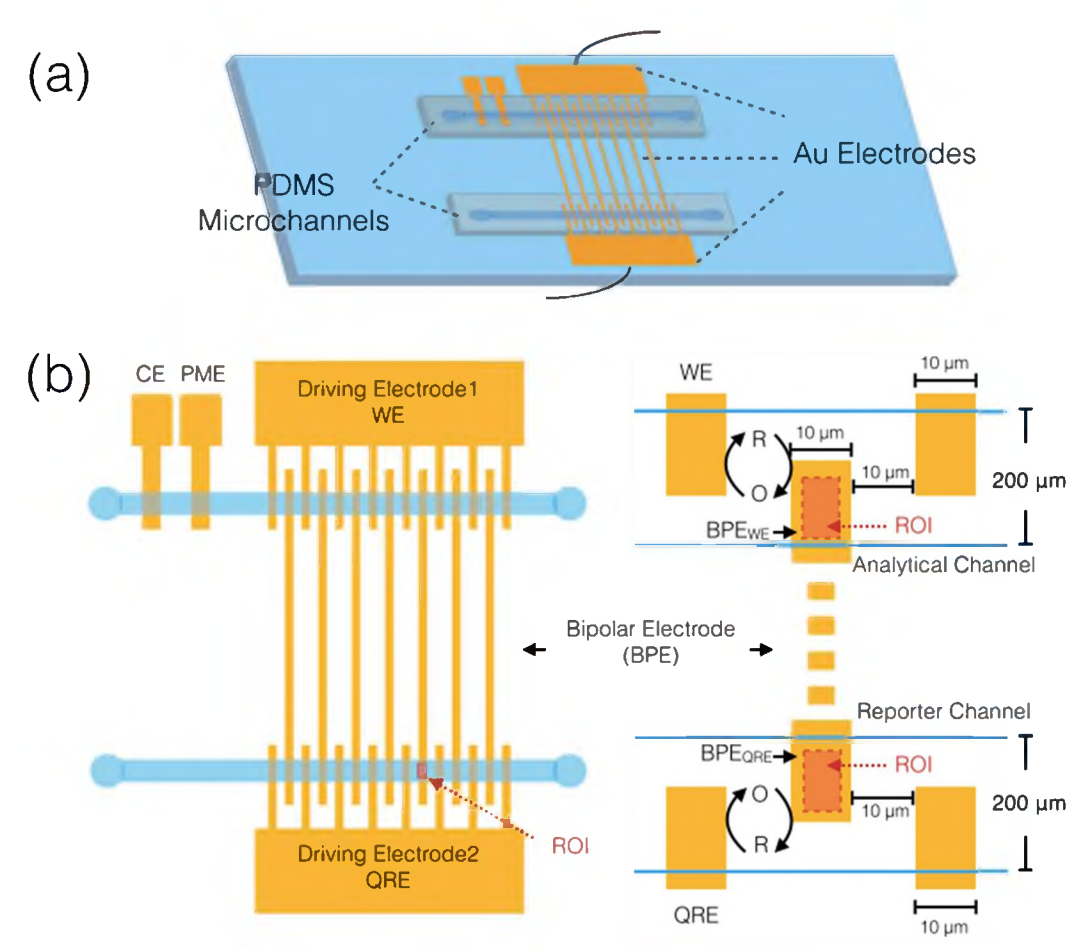
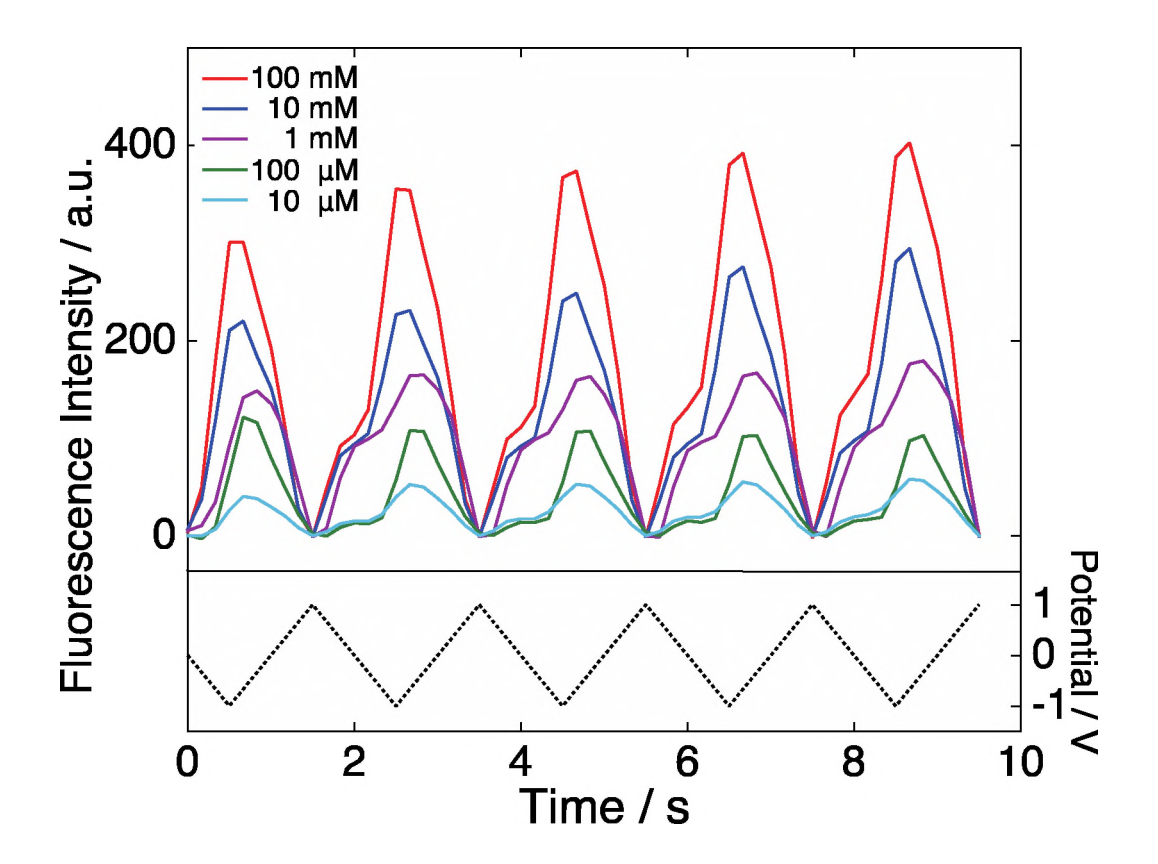
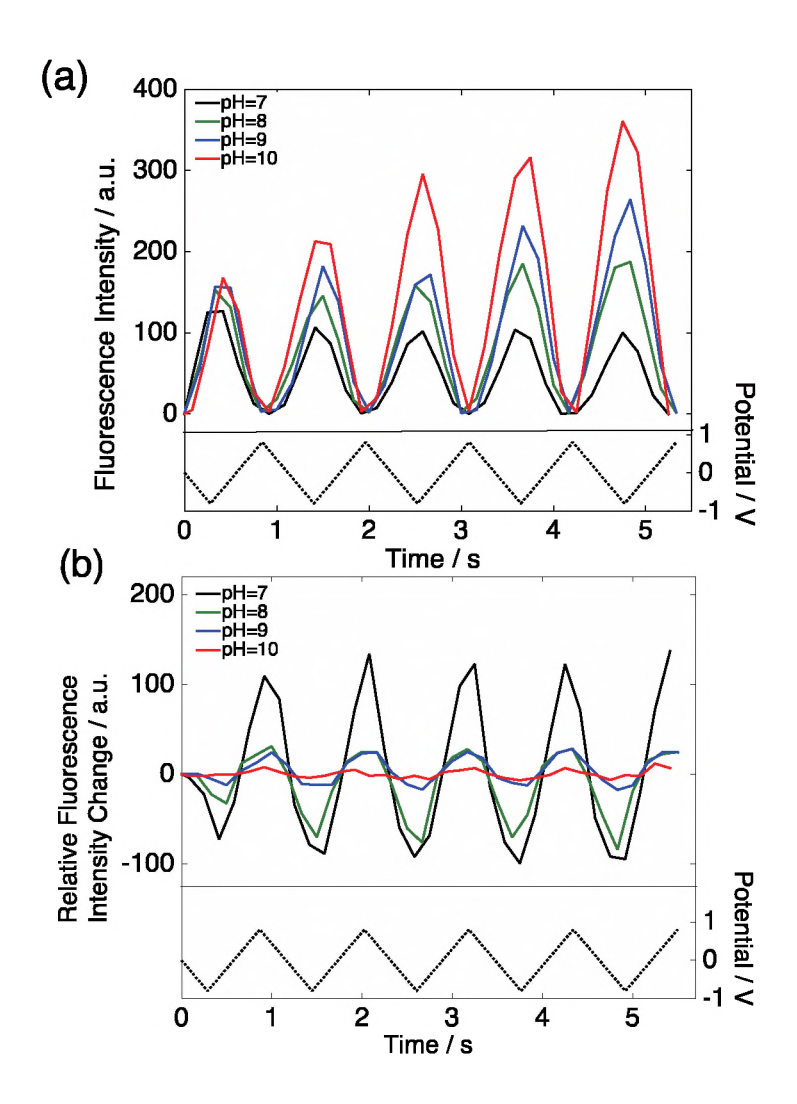


Figure 1. (a) Perspective view schematic illustration of the microfluidic bipolar electrode array device. (b) Schematic illustration of the mechanism of redox reaction coupling on a BPE array spanning two physically separated microchannels. (*Left*) Top view of the layout of the BPE array relative to the PME and the microfluidic channels. (*Right*) Top view at the opposite poles of a single BPE digit coupled to the WE digits in the analytical channel and to the QRE digits in the reporter channel. The regions of interest (ROI) used for fluorescence measurements are indicated on BPE<sub>WE</sub> and BPE<sub>QRE</sub>.



**Figure 2**. (*Top*) Fluorescence intensity as a function of time/potential in the reporter channel during the CV measurement of  $Fe(CN)_6^{3-}$  at different concentrations in the analytical channel. Fluorescence intensities represent region of interest (ROI - see Fig. 1) integrations of emission at the BPE<sub>QRE</sub>. (*Bottom*) Applied potential at WE as a function of time.



**Figure 3.** (*Top*) Fluorescence intensity as a function of time/potential during CV of QH<sub>2</sub> solutions at different pH values. (a) Resazurin/resorufin response in the reporter channel. Fluorescence intensities represent ROI (see Fig. 1) integrations of emission at the BPE<sub>QRE</sub>. (b) Fluorescein response in the analytical channel as a function of initial pH. Fluorescence intensities represent ROI integrations of emission at the BPE<sub>WE</sub>. (*Bottom*) Applied potential at WE as a function of time.

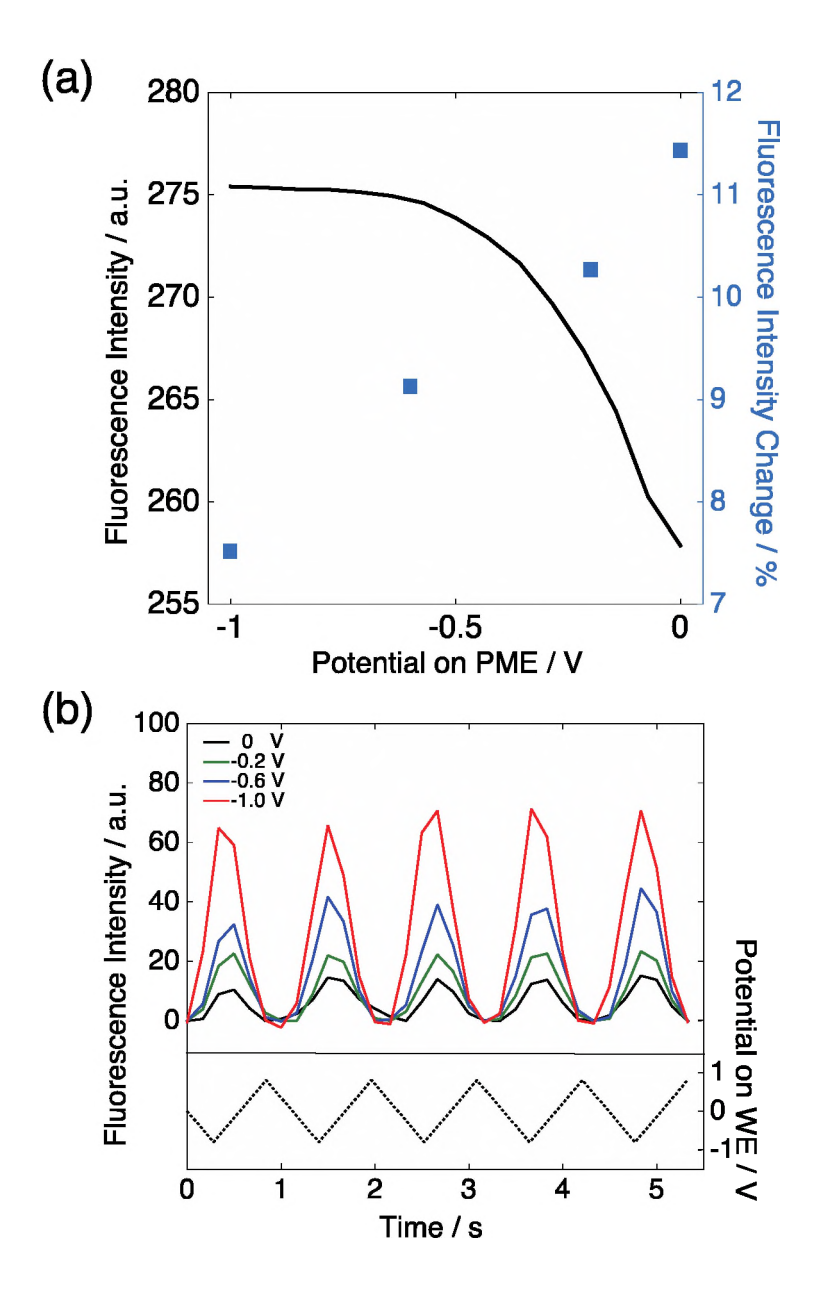


**Figure 4**. (a) Initial fluorescence intensity in the analytical channel as a function of PME potential (black curve) and its change during CV measurement of QH<sub>2</sub> in the analytical channel (blue squares). (b) Effect of PME potential (indicated by different colors) on the fluorescence intensity in the reporter channel during the CV measurement of QH<sub>2</sub> (10 mM, pH 7). (*Bottom*) Applied potential at WE as a function of time.

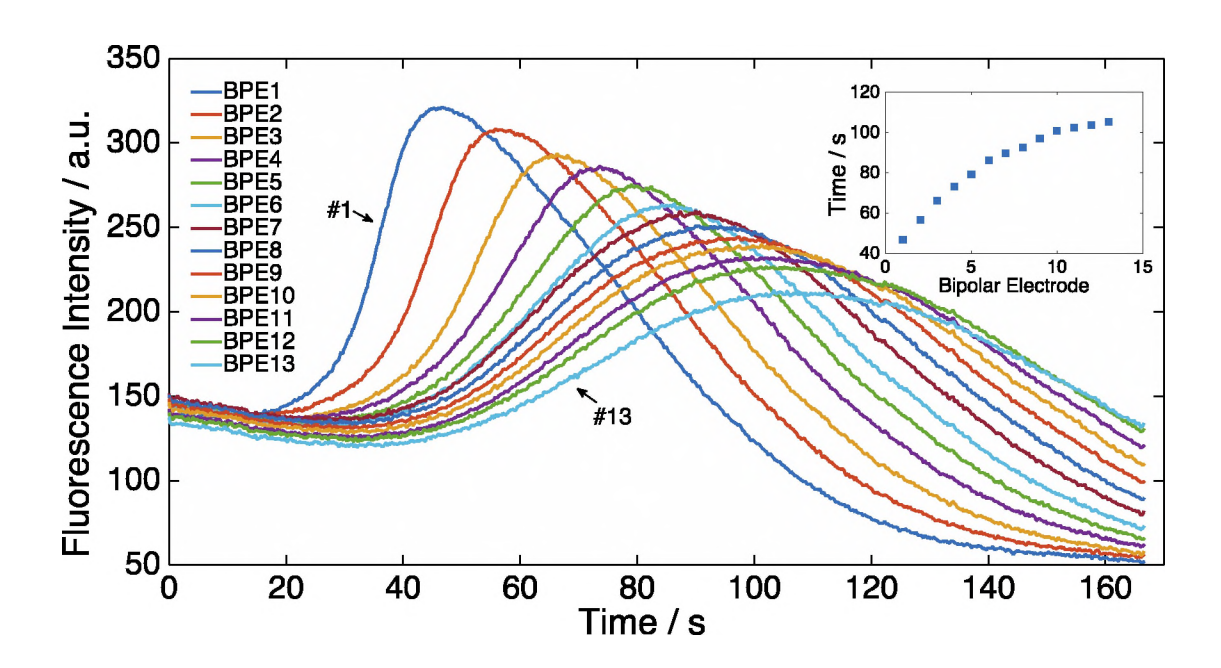


**Figure 5**. Fluorescence intensity as a function of time at different BPE digits in the analytical channel after a -1.0 V (*vs.* CE) potential pulse was applied to the PME. BPEs are numbered in order of their distance from the PME with BPE 1 being the closest and BPE 13 the farthest. (*Inset*) Time at which maximum fluorescence is observed at each BPE digit.

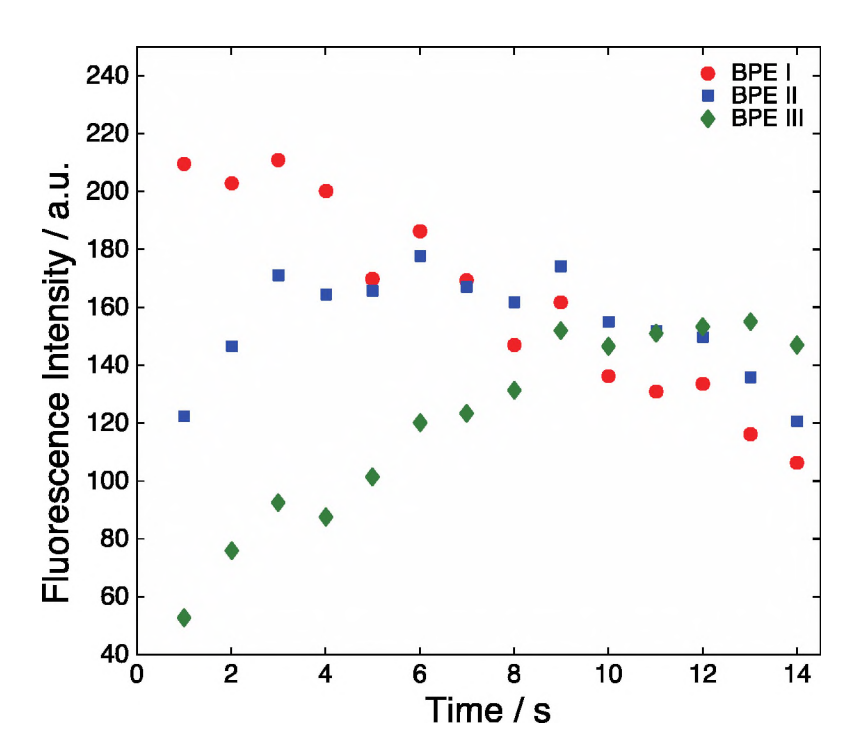


**Figure 6**. The fluorescence intensity of three representative BPEs in reporter channel varies with time in CV of QH<sub>2</sub> measured 45 s after a potential pulse (-1.0 V) was applied on PME. BPE I (red) and BPE III (green) are the closest and furthest to PME respectively, and BPE II (blue) is between BPE I and BPE III.

 Table 1. Electron Transfer Reaction Coupling in the Closed BPE Configuration.

	Analytical Channel (Analyte/ Fluorescein)		Reporter Channel (Resazurin/Resorufin)	
Potential on WE°	WE	$\mathrm{BPE}_{\mathrm{WE}}$	$\mathrm{BPE}_{\mathrm{QRE}}$	QRE
Negative	Reduction	Oxidation	Reduction*	Oxidation
Positive	Oxidation	Reduction	Oxidation	Reduction*

Relative to the equilibrium potential,  $E_{eq}$ . \*Accompanied by fluorescence emission.

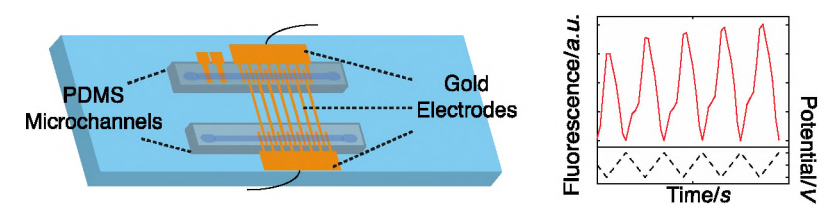


**Figure for the table of contents**. (*Left*) Perspective illustration of the microfluidic bipolar electrode array device. (*Right*) Fluorescence intensity as a function of time/potential in the re

# **Supplemental Information for**

Coupling of Independent Electrochemical Reactions and Fluorescence at Closed Bipolar Interdigitated Electrode Arrays

Wei Xu<sup>1</sup>, Chaoxiong Ma<sup>1</sup>, Paul W. Bohn<sup>1,2\*</sup>

The supplemental information below provides additional detail on the operation of the closed BPE architecture described in the body of the paper. Figure S1 is the complement to Fig. 2 and describes the behavior of the coupled closed BPE IDEA when Fe(CN)<sub>6</sub><sup>4-</sup> is used in the analytical channel, instead of Fe(CN)<sub>6</sub><sup>3-</sup>. Figure S2 shows the alternating pattern of bright and weak fluorescence emission on alternating BPE<sub>QRE</sub> and QRE digits under conditions in which the main analytical reaction at the WE is either oxidation of reduction. Figures S3 and S4 show the correspondence between the cyclic voltammetry at the working electrode in the analytical channel and the fluorescence measured in the reporter channel for 10 mM Fe(CN)<sub>6</sub><sup>3-</sup> (Figure S3) and 10 mM QH<sub>2</sub> (Figure S4).

<sup>&</sup>lt;sup>1</sup>Department of Chemistry and Biochemistry, University of Notre Dame, Notre Dame, IN 46556

<sup>&</sup>lt;sup>2</sup>Department of Chemical and Biomolecular Engineering, University of Notre Dame, Notre Dame, IN 46556

<sup>\*</sup>Author to whom correspondence should be addressed, pbohn@nd.edu

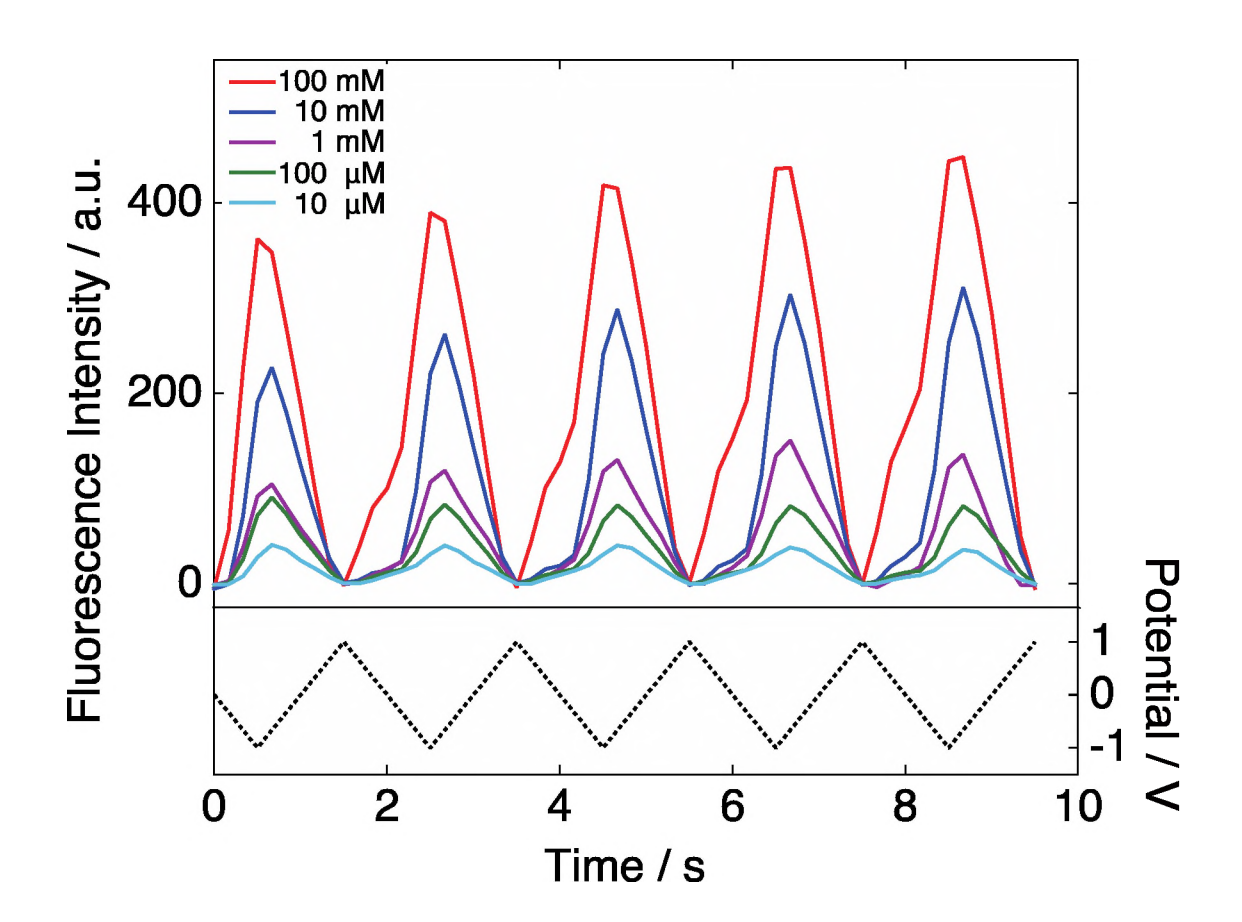


**Figure S1**. Fluorescence intensity as a function of time/potential in the reporter channel during the CV measurement of  $Fe(CN)_6^{4-}$  at different concentrations in the analytical channel. Fluorescence intensities represent ROI integrations of emission at the BPE<sub>QRE</sub>. (*Bottom*) Applied potential at WE as a function of time.

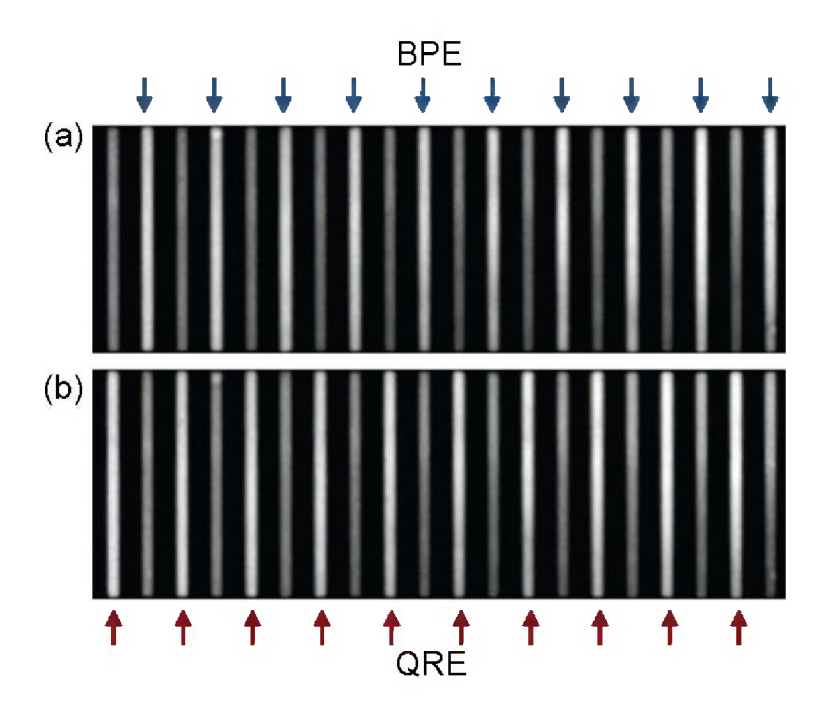


Figure S2. Fluorescence microscopy image of QRE/BPE IDEA in reporter channel during redox of chemistry of 10 mM QH<sub>2</sub> at the WE. (a) cathodic potential applied to WE (BPEs are bright); b) anodic potential applied to WE (QRE are bright) in the CV measurement. Blue and red arrows denote BPE<sub>QRE</sub> and QRE digits, respectively.

29

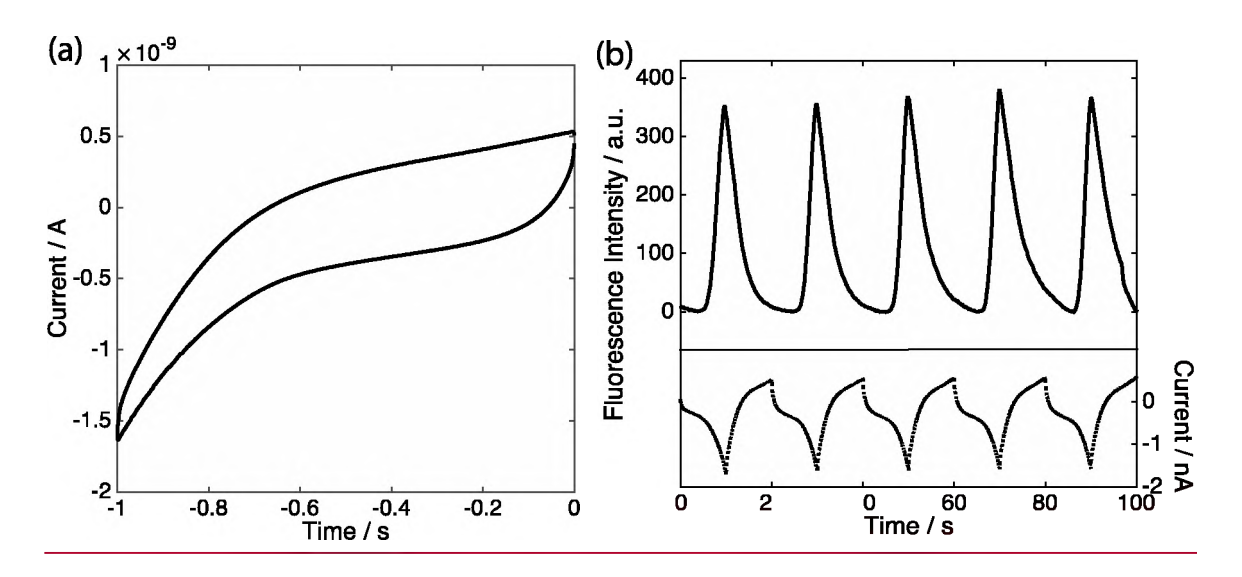


Figure S3. (a) Cyclic voltammetry of  $10 \text{ mM Fe}(\text{CN})_6^{3-}$  at scan rate of 0.1 V/s. (b) (Top)Fluorescence intensity as a function of time in the reporter channel during CV measurement of  $10 \text{ mM Fe}(\text{CN})_6^{3-}$  in the analytical channel. (*Bottom*) Current at WE as a function of time.

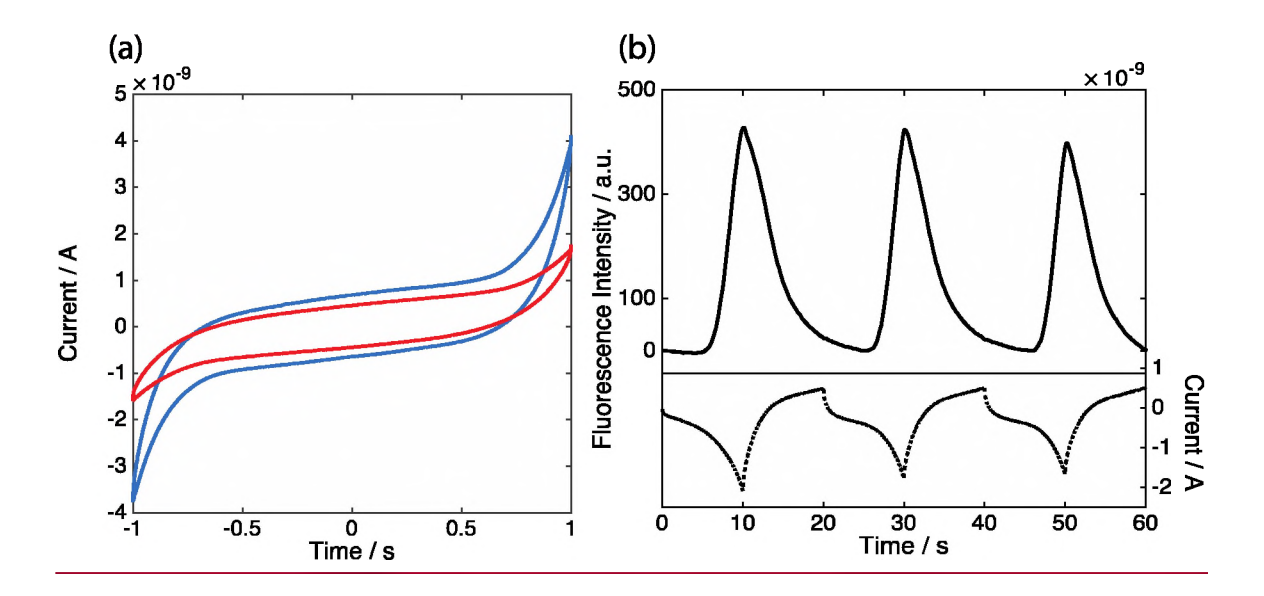


Figure S4. (a) Cyclic voltammetry of 10 mM QH<sub>2</sub> at pH = 7 (red) and pH = 9 (blue) with scan rate at 0.1 V/s. (b) (Top) Fluorescence intensity as a function of time in the reporter channel during CV measurement of 10 mM QH<sub>2</sub> in analytical channel. (Bottom) Current at WE as a function of time.

porter channel during cyclic voltammetry.